Quench characteristics of 6 T conduction-cooled NbTi magnet system

S Kar[1,3],V Soni[2], P Konduru[1], R G Sharma[1] , D Kanjilal[1] and T S Datta[1]

[1]Inter-University Accelerator Centre, New Delhi,110067, India
[2]National Institute of Technology, Rourkela, Odisha, India

E-mail: kar.soumen@gmail.com

Abstract. Conduction-cooled superconducting magnets are cooled by cryocooler alone through the conductive thermal links. The limited refrigeration capacity and conductive cooling make the magnets more prone to quench. We have studied the quench characteristics of a 6 T conduction-cooled NbTi magnet system in detail in this paper. The NbTi magnet has been designed for 102 A with 31% current margin to achieve 0.8 K temperature margin. During a training quench at 101.2 A, the outer surface of the NbTi magnet reached 53.25 K and the temperature of the 2nd stage cold head of the cryocooler reached 15.8 K. Conductive cooling by the cryocooler makes the post-quench recovery of the NbTi magnet in 40 minutes. The maximum sweep rate is 6 A/min for thermally stable operation of this conduction-cooled NbTi magnet. We have done an intentional quench at a sweep rate of 8 A/min. The maximum hot-spot temperature and the post-quench current decay have been simulated using a finite element analysis (FEA) code. Post-quench distribution of the dumped energy in the different components of the magnet system is also presented.

1. Introduction

Cryogen-free magnets are cooled using a cryocooler alone through the conductive thermal links. In a conduction-cooled magnet, any small thermal perturbation would be reflected by the rise in the temperature of the magnet. Conduction-cooled NbTi magnet is thus more prone to quench compared to bath cooled magnet even though, the inter-layer heat transfer in the winding is through the conduction process in both types of magnets, both being fully epoxy impregnated [1].

One of the important features of any conduction-cooled NbTi magnet is to achieve thermal stability against any thermal disturbance. The pattern of temperature rise of any conduction-cooled magnet greatly depends on the operational heat loss (e.g. AC loss, Ohmic heat loss etc.) profile [2-4]. Hence, thermal stability of the conduction-cooled magnet will be governed by the energy balance at the magnet which is given by (1),

$$mC_p \frac{dT_{mag}}{dt} = Q_{Heating} - Q_{Cooling} \quad (1)$$

where m , C_p are the mass of the magnet and average specific heat of the NbTi and copper of the magnet, t is time and T_{mag} is the temperature of the magnet, $Q_{Heating}$ is the heat generation during

[3] To whom any correspondence should be addressed.

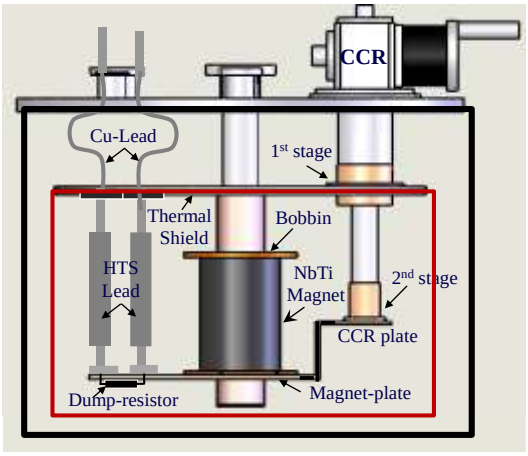

Figure 1. Schematic of the 6 T conduction-cooled NbTi magnet system

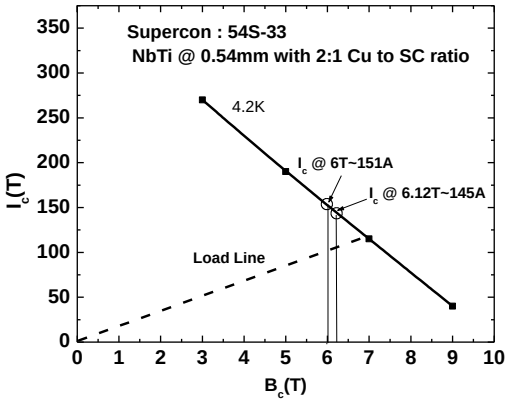

Figure 2. Operational load line of the 6 T NbTi magnet.

operation of the magnet and $Q_{Cooling}$ is the effective cooling by the cryocooler through the conductive links.

For a superconducting magnet, current sharing temperature limits its operational temperature margin [5]. The temperature of a NbTi magnet (T_{mag}) has to be lower than its current sharing temperature (T_{cs}) for stable operation. A quench in a conduction-cooled NbTi magnet may occur because of numerous reasons and one or more types of quench can simultaneously take place during its operation [6-7]. It is necessary to prevent overheating of the NbTi magnet as the entire stored energy of the NbTi magnet will be distributed in the magnet system after any type of quench.

Quench characteristics has been studied for the conduction-cooled 6 T NbTi magnet system developed at Inter-University Accelerator Centre, New Delhi [8]. Figure 1 shows the schematic of the 6 T conduction-cooled NbTi magnet system. A two stage GM cryocooler (SHI cryogenics, SRDK-415D) of refrigeration capacity of 1.5 W at 4.2 K has been used in the magnet system. The magnet is cooled by the cryocooler through conductive thermal links. During a quench, the dissipated heat in the magnet will be conducted to the cryocooler through the thermal links. A finite element analysis (FEA) code has been used for the magnet to simulate the maximum hot-spot temperature along with the transient thermal map and its post-quench current decay.

2. Load line and temperature margin

To design the 6 T NbTi solenoid magnet, it is essential to define its operational load line which defines the operation margins for the magnet [9]. Figure 2 shows critical current versus the magnetic field for the NbTi conductor (Supercon Inc.) used for the magnet. The critical current of the multi-filamentary NbTi conductor used for the magnet is 151 A at the central field (B_0) of 6 T. The peak field (B_P) on the conductor is however, 6.12 T. The corresponding critical current is 145 A . The load line as shown in figure 2 has been chosen based on the peak field in the magnet. The operating current has been chosen 102 A keeping a current margin of 31% which eventually gives 0.8 K margin of temperature, as the estimated current sharing temperature will be 5 K for the magnet at 6 T field operated at 4.2 K [5]. The parameters of the magnet has been summarized in table 1.

During a quench, the dissipated heat energy would adiabatically raise the temperature of the magnet which eventually depends on the specific heat of the composite NbTi conductor. Using the temperature dependent function of specific heat of the NbTi and the copper [10], the specific heat of the composite conductor with 2:1 copper to superconductor ratio has been estimated to be 2 mJ/cm^3-K at 4.2 K operating temperature. Energy of couple of millijoule is required to raise the temperature of the 1 cm^3 volume of the composite conductor from 4.2 K to the estimated current sharing temperature

Table 1. Parameters of the 6 T NbTi magnet

Description	Value
Magnetic field at centre	6 T
Peak magnetic field	6.12 T
Operating current	102 A
Inner diameter	104 mm
Outer diameter	137 mm
Winding length	200 mm
Diameter of NbTi conductor	0.54 mm
Cu: NbTi	2:1
Inductance	5.5 H
Parallel dump resistor	5 Ω
Stored energy at 6 T	28 kJ

of 5 K. Hence, very minimal amount of external heat would be sufficient to drive the composite conductor from its superconducting state to normal state.

3. Quenching of magnet and analysis

3.1. Quench protection

Any potted-magnet may quench during its operation, so it is essential to protect the magnet. A non-inductively wound 5 Ω resistor has been used in parallel to the magnet which has an inductance of 5.5 H. In a conduction-cooled magnet system, it is also necessary to protect the magnet in the event of burnt out or breaking of the HTS current lead. Hence, a parallel dump resistor has been thermally fixed to the magnet-plate as shown in figure1. Though, cold diodes have not been used , as the power dissipation on the dump resistor will be 50-60 mW during charging or discharging of the magnet at a sweep rate of 6 A/min which is the maximum sweep rate for this magnet for its stable operation [8]. During its steady state operation, the voltage across the magnet becomes negligible. Hence, there is no continuous heat dissipation on the dump resistor.

3.2. FEA simulation of quench

To simulate a quench in the magnet, a 3-D model of the entire solenoid has been used in the FEA analysis with the commercial software OPERA (Vector Field) [11]. The initial temperature of the magnet has been considered to be 4.2 K in the quench simulation. The protection circuit in the FEA analysis has been defined with 5 Ω parallel resistor.

Figure 3 shows the post-quench current decay profile simulated for the magnet quenched at 102 A . The current decays to 50% of its value within 250 ms and it decays to zero in 1 s after the quench. The current decay of the magnet is determined by the effective resistance in the electrical equivalent protection circuitry. Figure 4 shows the transient thermal profile of the magnet after 0.1 s of quenching at 102 A. It also shows that the temperature of most parts of the magnet is more than 5 K whereas the hot spot temperature is approximately 62 K. During a quench, the normal zone grows and the resistance of the magnet increases. Figure 5 shows the transient thermal profile of the magnet after 1 s of quenching at 102 A. The maximum hot spot temperature simulated for the magnet is found to be 73.3 K at 1 s after quench and the minimum temperature of the magnet is 25 K as shown in figure 5. Hence, the

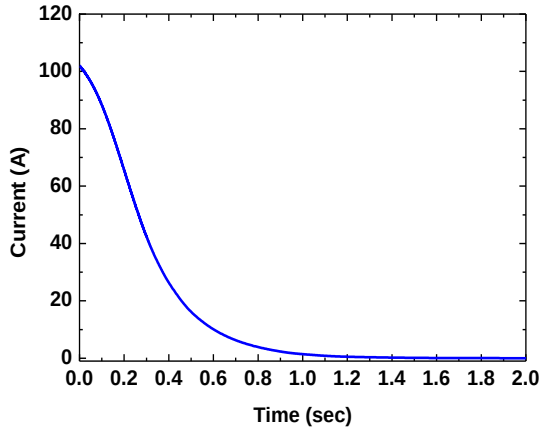

Figure 3. Post-quench current decay simulated for the 6 T NbTi magnet using OPERA (Vector Field) FEA code.

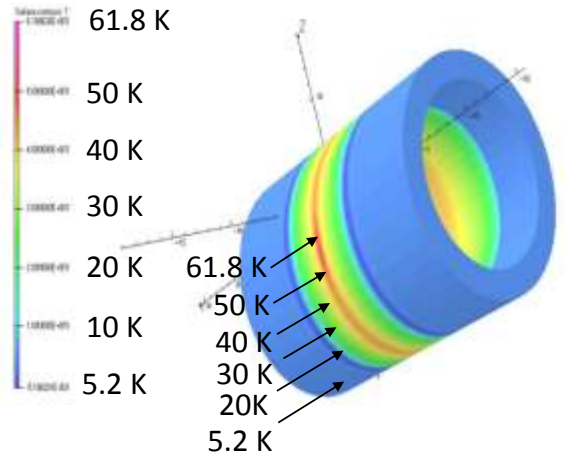

Figure 4. Post-quench transient thermal mapping at 0.1 s simulated for the 6 T NbTi magnet using OPERA (Vector Field) FEA code.

average temperature simulated for the magnet is approximately 50 K. The corresponding overall resistance growth is 25.3 Ω in 1 s. This resistance will play significant role in determining the post-quench energy distribution in the magnet and the dump resistor.

3.3. Quenching of the NbTi magnet

During operation, the thermal profile of different components of the magnet system has been measured by calibrated Cernox (Lakeshore Cryotronics Inc.) sensors. A calibrated Cernox sensors has also been fixed on the outer surface of the magnet winding using Stycast epoxy. Figure 6 shows the post-quench thermal profile of different components of the magnet system. The magnet quenched at 101.2 A. This represents a training quench which happened during the first energization of the conduction-cooled solenoid magnet.

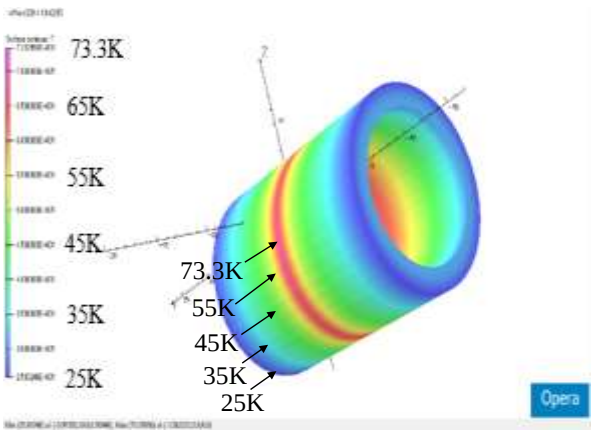

Figure 5. Post-quench transient thermal mapping after 1 s simulated for the NbTi magnet using OPERA (Vector Field) FEA code.

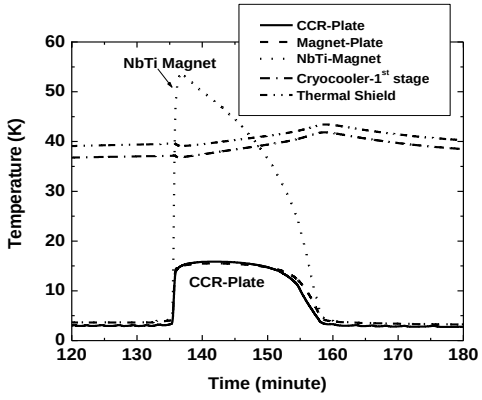

Figure 6. Measured thermal profile of the NbTi magnet quenched at 101.2 A: NbTi-magnet temperature has been measured at the outer surface of the winding.

This figure shows an adiabatic rise in temperature of various components of the magnet system after the quench. The temperatures at outer surface of the magnet and the CCR-plate have been reached to 53.25 K and 15.8 K respectively. Though, the hot-spot temperature inside the winding of the magnet will be much higher. The temperature measured at the outer surface of the magnet is closely matching with average temperature simulated using OPERA.

The magnet returns to 3.9 K after 25 minutes of the quenching and then 3.3 K after 40 minutes. Figure 6 also shows how the thermal shield and the 1st stage of the cryocooler behaves after the quenching. After quenching, temperature of the thermal shield starts increasing slowly till the CCR-plate reaches to the 3.3 K from 15.8 K. This increment in the temperature of the thermal shield is due to sudden reduction in the refrigeration capacity of the 1st stage of the cryocooler after an adiabatic transition in the load map. The rise of the temperature is of the order of 5 K in 40 minutes.

After a training quench, the magnet has been re-energized to 102 A to achieve 6 T central field. The maximum sweep rate for this magnet system is 6 A/min (0.36 T/min) for its thermally stable operation [8]. To see the effect of higher sweep rates, the magnet has been energized with 8 A/min (0.47 T/min) sweep rate to quench it intentionally. The magnet has been quenched at 14 A (~0.82 T) while energizing at 8 A/min sweep rate. The temperature of the magnet has been raised to 14.35 K whereas the magnet-plate to 10.2 K and the CCR-plate to 8.1 K. It is evident for any conduction-cooled magnet system, the energy balance between the dynamic heat generation and effective cooling by the cryocooler through the conductive links plays a crucial role in limiting the sweep rate. In case of a bath cooled magnet, the maximum sweep rate could have been much higher for the same solenoid magnet.

3.4. Quench energy distribution

During a quench, the stored energy (E_{Total}) will be dumped adiabatically in the magnet including the parallel dump resistor. The deposited heat energy will eventually raise the temperature of the magnet. The total energy deposited is given by (2),

$$E_{Total} = E_{mag} + E_{dump} \tag{2}$$

where E_{mag} and E_{dump} are the energies dumped in the magnet and the dump resistor respectively. The stored energy (E_{Total}) of the magnet at 101.2 A is 28 kJ.

Similarly, the total resistance in the circuit can be expressed as the sum of the resistance grown in the magnet (R_{mag}) and the dump resistance (R_{dump}) and is given by (3),

$$R = R_{mag} + R_{dump} \tag{3}$$

Here, the value of dump resistor (R_{dump}) used in the protection circuit is 5 Ω and the post-quench resistance (R_{mag}) simulated for the magnet is 25.3 Ω.

The fraction of energy (E_f) dumped in the magnet would depend on the ratio of the dump resistor and the resistance grown inside the magnet during a quench. The fraction of energy dumped in the magnet which is given by (4),

$$E_f = \frac{R_{mag}}{R_{mag} + R_{dump}} = \frac{E_{Total} - E_{dump}}{E_{Total}} \tag{4}$$

Using (2)-(4), the fractional energy (E_f) dumped in the magnet is estimated to be 83% which corresponds to 23 kJ. Rest of the stored energy (17 %) is dissipated in the dump resistor.

The energy dumped in the magnet will adiabatically be distributed in the different associated components (like magnet-plate, CCR-plate) thermally connected with the magnet. The amount of heat energy dissipated on the magnet and other associated components could be estimated using their instantaneous temperature rise (ΔT) and heat capacity (C_p) value of the corresponding material. The dissipated heat energy (Q_d) is given by,

$$Q_d = \int_4^{54} \left(m_{Cu-matrix} C_P^{CU} + m_{NbTi} C_P^{NbTi}\right) dT + \int_4^{54} \left(m_{Stycast} C_P^{Stycast}\right) dT + \int_4^{16} \left(\left(m_{bobbin} + m_{mag-plate} + m_{CCR-plate} + m_{Cu-Strips}\right) C_P^{CU}\right) dT + \int_4^{16} \left(m_{SS-bolts} C_P^{SS}\right) dT \quad (5)$$

where $m_{Cu-matrix}$, m_{NbTi}, $m_{Stycast}$ are the masses of copper matrix in NbTi wire, NbTi and Stycast epoxy and m_{bobbin}, $m_{mag-plate}$, $m_{Cu-strips}$, $m_{SS-bolt}$ respectively are the masses of the magnet bobbin, magnet-plate, cooling strips made of ETP copper and mass of SS-bolts used for fastening the components and C_p^{Cu}, C_p^{NbTi}, $C_p^{Stycast}$ and C_p^{SS} are the specific heat respectively for the copper, NbTi, Stycast and SS304.

The specific heats of copper and NbTi are the temperature dependent functions [10]. Using (5), the energy dissipation after quenching at 101.2 A, on the magnet and other associated components connected at the 2nd stage of the CCR, is estimated to be approximately 22 kJ which is 78 % of the stored energy of the magnet at 101.2 A. The remaining 22% of energy has been dissipated in the dump resistor. Hence, the measured energy dumped (78%) in the magnet and its associated components deviates by 5% with the estimated fractional energy (83%) dump. This deviation might be due to improper estimation of thermal masses of the different associated components.

3.5. Recovery after quench

During a quench, though the temperature rise of the magnet is instantaneous (less than a second) because of adiabatic dumping of the stored energy. But, post-quench recovery of the magnet is very slow (tens of minutes) in the conduction-cooled system. The dissipated heat energy in the magnet and the associated components is taken out solely by the cryocooler though the conductive links. The dump resistor is mounted on the magnet-plate (shown in figure 1) which is thermally connected to the 2nd stage of the cryocooler. Hence, the entire stored energy dissipated needs to be taken out only by the cryocooler. Limited refrigeration capacity of the 2nd stage of the cryocooler takes longer time to take out the stored energy which is in our case, 28 kJ at 101.2 A. Figure 7 shows the expanded view

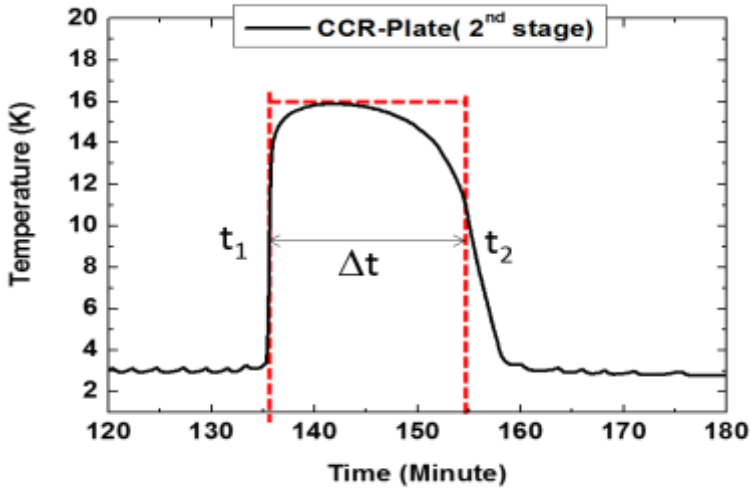

Figure 7. Post-quench temperature profile of the CCR-plate of the 2nd stage of the cryocooler.

of the thermal profile (shown in the figure 6) of the CCR-plate after a quench at 101.2 A. The total thermal energy extracted (Q_{CCR}) by the cryocooler is estimated by using (6) which is given by ;

$$Q_{CCR} = -\int_{t1}^{t2} R(T)dt \approx R\Delta t \quad (6)$$

where negative sign indicates the cooling, $R(T)$ is the temperature dependent refrigeration capacity of the cryocooler at temperature T at CCR-plate and $\Delta t = t2 - t1$ signifies the time duration of the post-quench refrigeration. To simplify the calculation, the temperature of the CCR-plate is considered to be as a constant for the time period of Δt as shown in figure 7.

The temperature at the CCR-plate remains at 15.8 K for 18-20 minutes before starting to reduce. The refrigeration capacity of the 2nd stage of the cryocooler at that temperature is found to be 18 W estimated from the cryocooler load map [12]. The heat energy extracted by the cryocooler is estimated to be 24 kJ which is 15% less than the total stored energy of the magnet. This variation might be due to the approximation made in estimation of the refrigeration capacity of the cryocooler.

4. Conclusion

The thermal stability of conduction cooled magnet system against any thermal eventuality is poor in comparison to the bath-cooled magnets, even though, the inter layer heat transfer in the epoxy impregnated winding is through the conduction only in both cases. Unlike bath cooled magnet, the limited refrigeration capacity of the 2nd stage of the cryocooler and conductive cooling through the thermal links make the post-quench recovery time longer for the magnet. Quenching of the magnet at 8 A/min sweep rate signifies the energy imbalance between the dynamic heat generation and the conductive cooling for this NbTi magnet system To increase the sweep rate, the conductance of the thermal link between the magnet and cryocooler needs to be improved.

Acknowledgments

Authors would like to thank the Department of Science and Technology, Govt. of India for giving the financial support to carry out the study. Authors would also like to thanks the personnel of the cryogenic group for their technical support toward this project.

References

[1] Turowski P 1992 *IEEE Transactions on Magnetics* MAG-**15 (1)** 1979
[2] Watanabe K *et al.*1996 *Cryogenics* **36** 1019
[3] Hongwei L *et al.*2005 *IEEE Transactions of Applied Superconductivity* **15(2)** 1699
[4] Rabbers J J *et al*. 2006 *IEEE Transactions of Applied Superconductivity* **16(2)** 549
[5] Meβ K H 1989 *Proc. CERN Accelerator School,* **CERN 89-04** 87
[6] Iwasa Y 2005 *IEEE Transactions on Apllied Superconductivity* **15(2)** 1165
[7] Bottura L 2013 *Pro. of the WAMSDO:Workshop on Accelerator Magnet Superconductor,Deisgn and Optimizatio*n **CERN-2013-006** 1
[8] Kar S et al. 2012 *Cryogenics* **52(12)** 739
[9] Wilson M N 1986 *Superconducting Magnets* (Oxford: Oxford University Press)
[10] Kim S W 2000 FNAL **TD note 00-41** Batavia.
[11] http://www.cobham.com/media/637229/cts_vectorfields_opera_240610.pdf
[12] Datasheet of SRDK-415 cryocooler; http://www.shicryogenics.com.